

¹H NMR, EPR, UV–Vis, and Electrochemical Studies of Imidazole Complexes of Ru(III). Crystal Structures of *cis*-[(Im)₂(NH₃)₄Ru^{III}]Br₃ and [(1MeIm)₆Ru^{II}]Cl₂·2H₂O

M. J. Clarke,^{*,†} V. M. Bailey,[†] P. E. Doan,^{*,‡} C. D. Hiller,[†] K. J. LaChance-Galang,^{†,§} H. Daghlian,[†] S. Mandal,[†] C. M. Bastos,^{||} and D. Lang[†]

Merkert Chemistry Center, Boston College, Chestnut Hill, Massachusetts 02167,
Department of Chemistry, Northwestern University, Evanston, Illinois 60208, and Procept, Inc.,
Cambridge, Massachusetts 02139

Received April 3, 1996[⊗]

Comparisons of the spectroscopic properties of a number of Ru^{III} complexes of imidazole ligands provide methods of distinguishing between various types of bonding that can occur in proteins and nucleic acids. In particular, EPR and ¹H NMR parameters arising from the paramagnetism of Ru^{III} should aid in determining binding sites of Ru^{III} drugs in macromolecules. Electrochemical studies on several imidazole complexes of ruthenium suggest that imidazole may serve as a significant π -acceptor ligand in the presence of anionic ligands. Crystal structures are reported on two active immunosuppressant complexes. *cis*-[(Im)₂(NH₃)₄Ru^{III}]Br₃ crystallizes in the triclinic space group *P* $\bar{1}$ (No. 2) with the cell parameters $a = 8.961(2)$ Å, $b = 12.677(3)$ Å, $c = 7.630(2)$ Å, $\alpha = 98.03(2)^\circ$, $\beta = 100.68(2)^\circ$, $\gamma = 81.59(2)^\circ$, and $Z = 2$ ($R = 0.044$). [(1MeIm)₆Ru^{II}]Cl₂·2H₂O crystallizes in the monoclinic space group *P*2₁/*n* (No. 14) with the cell parameters $a = 7.994(2)$ Å, $b = 13.173(4)$ Å, $c = 14.904(2)$ Å, $\beta = 97.89(1)^\circ$, and $Z = 2$ ($R = 0.052$). The average Ru^{II}–N bond distance is 2.106(8) Å.

Introduction

Ruthenium complexes with imidazole ligands are of interest for their antitumor activity,^{1,2} for their ability to ligate radiosensitizing agents to DNA,³ and as models for the covalent bonding of ruthenium to nucleic acids, which occurs most frequently on the imidazole ring of guanine.^{3–5,6} More recently, *cis*-[(His)₂(NH₃)₄Ru^{III}] has been employed as a bridge between histidyl imidazoles to stabilize polypeptide α -helices,⁷ with molecular mechanics calculations suggesting that the metal may cross-link through either the N _{ϵ} or the more sterically hindered N _{δ} site on the imidazole ring.⁸ There is also convincing evidence that the core of the antitumor agent *trans*-[Cl₄(Im)₂-Ru], binds to an imidazole in transferrin as it is transported to the tumor site.⁹ Finally, the recent discovery that nanomolar concentrations of stable ruthenium(III) complexes with nitrogen and nitrogen heterocyclic ligands inhibit the antigen-independent phase of T cell proliferation points toward an exciting new class of immunosuppressive agents that are unlike cyclosporin A and FK506.¹⁰

Consequently, the spectroscopic parameters of ruthenium complexes with imidazole ligands are important in characterizing the biological interactions of this metal. The contact and dipolar NMR shifts of the imidazole H5 proton in the series *trans*-[L(Im)(NH₃)₄Ru^{III}] have been previously calculated from NMR, EPR, and crystallographic data. In these complexes, the magnetic resonance spectra are strongly dependent on the π -donor/acceptor characteristics of L and reveal a surprising correlation between reduction potentials and the difference between the two largest EPR g values.¹¹

In some cases, complexes thought to be *cis*-coordinated imidazoles¹² or purines¹³ have been reported, but they have resulted from preparations of carbon-bound ligands, which are known to labilize the *trans* position. Describing the spectroscopic properties of well-characterized imidazole complexes of Ru^{III}, especially those containing *cis*- and *trans*-imidazoles, should provide models for probing ruthenium binding and cross-linking in both proteins and nucleic acids. Herein, we report on the following: (1) the magnetic resonance spectra of [(L)-(NH₃)₅Ru]³⁺, where L is imidazole or methylimidazole, in order to accurately assign resonances; (2) a comparison of the spectroscopic properties of *cis*- and *trans*-[(Im)₂(NH₃)₄Ru]³⁺ and related complexes; (3) the crystal structures of the immunosuppressants *cis*-[(Im)₂(NH₃)₄Ru^{III}]Br₃ and [(1MeIm)₆Ru^{II}]Cl₂·2H₂O; (4) electrochemical studies on Ru^{III} imidazole complexes that bear on their likely oxidation state in biological environments.

Experimental Section

Syntheses. RuCl₃ was purchased from Johnson Matthey. *cis*-[Cl₂(NH₃)₄Ru]Cl,⁶ *trans*-H[Im][Cl₄(Im)₂Ru],¹⁴ and [L(NH₃)₅Ru]Cl₃, where

[†] Department of Chemistry, Boston College.

[‡] Department of Chemistry, Northwestern University

[§] Presently at Regis College, Weston, MA.

^{||} Procept Inc.

[⊗] Abstract published in *Advance ACS Abstracts*, July 15, 1996.

- Clarke, M. J. *Ruthenium and Other Non-Platinum Metal Complexes in Cancer Chemotherapy*; Springer-Verlag: Heidelberg, Germany, 1989; Vol. 10.
- Keppler, B. K. *Metal Complexes in Cancer Chemotherapy*; VCH: Weinheim, Germany, 1993, p 429.
- McNamara, M.; Clarke, M. J. *Inorg. Chim. Acta* **1992**, *195*, 175–185.
- Clarke, M. J.; Jansen, B.; Marx, K. A.; Kruger, R. *Inorg. Chim. Acta* **1986**, *124*, 13–28.
- Clarke, M. J.; Stubbs, M. *Met. Ions Biol. Syst.* **1996**, *32*, 727–780.
- Dhubhghaill, O. M. N.; Hagen, W.; Keppler, B. K.; Lipponer, K.-G., L.; Sadler, J. J. *Chem. Soc., Dalton Trans.* **1994**, 3305–3311.
- Ghadiri, M. R.; Fernholz, A. K. *J. Am. Chem. Soc.* **1990**, *112*, 9633–35.
- Choma, C. T.; Lear, J. D.; Nelson, M. J.; Dutton, P. L.; Robertson, D. E.; DeGrado, W. F. *J. Am. Chem. Soc.* **1994**, *116*, 856–865.
- Kratz, F.; Keppler, B. K.; Messori, L.; Smith, C.; Baker, E. N. *Met.-Based Drugs* **1994**, *1*, 169–173.

(10) Bastos, C. M.; Ocain, T. D.; Gordon, K. A.; Sampo, T. M.; Clarke, M. J.; Daghlian, H. *Abstracts of Papers*, 211th National Meeting of the American Chemical Society, New Orleans, LA, Spring 1996; American Chemical Society: Washington, D.C., 1996; INOR 582.

(11) LaChance-Galang, K. J.; Doan, P. E.; Clarke, M. J.; Rao, U.; Yamano, A.; Hoffman, B. *J. Am. Chem. Soc.* **1995**, *117*, 3529–3538.

(12) Sundberg, R. J.; Bryan, R. F.; Taylor, I. F.; Taube, H. *J. Am. Chem. Soc.* **1974**, *96*, 381–92.

(13) Clarke, M. J.; Taube, H. *J. Am. Chem. Soc.* **1975**, *97*, 1397–1403.

L = imidazole, 1-methylimidazole (1MeIm), 2-methylimidazole (2MeIm), and 5-methylimidazole (5MeIm),^{12,14} were prepared by literature methods. Anal. Calcd for [(2MeIm)(NH₃)₅Ru]Cl₃·2H₂O: C, 11.70; H, 6.14; N, 23.87; Cl, 25.90. Found: C, 11.77; H, 6.41; N, 23.52; Cl, 25.75. The reaction of 4-methylimidazole (4MeIm) with [H₂O(NH₃)₅Ru]²⁺, which was air-oxidized and purified by chromatographic separation on a Dowex-50 ion-exchange column to yield [(5MeIm)(NH₃)₅Ru]Cl₃, consistently showed a second set of NMR resonances, which tentatively was attributed to a small amount of the other linkage isomer, [(4MeIm)(NH₃)₅Ru]Cl₃ (δ (H₂), -20.7; δ (H₅), -2.3; δ (CH₃-4)) 14.8).

cis-[(Im)₂(NH₃)₄Ru]Cl₃ was prepared by reduction of *cis*-[Ru(NH₃)₄Cl₂]Cl¹⁵ with zinc amalgam under an argon atmosphere in the presence of a 4-fold excess of imidazole for 3 h. The zinc was then removed, and the resulting greenish-yellow solution was oxidized with a 50/50 mixture of 30% H₂O₂/3 M HCl until it turned orange. Addition of acetone precipitated an orange solid, which was dissolved in water and loaded onto an SP-C50-Sephadex ion-exchange column. The desired orange band eluted with 0.4 M HCl was subjected to rotary evaporation and dissolved in a minimum of water. Vapor diffusion of acetone into the solution afforded crystals. Anal. Calcd for [(Im)₂(NH₃)₄Ru]Cl₃: C, 17.50; H, 4.91; N, 27.22; Cl, 25.83. Found: C, 17.75; H, 4.73; N, 27.19; Cl, 25.86. UV-vis (λ_{\max} nm (ϵ M⁻¹ cm⁻¹)): 286 (1390); 310 (1914); 438 (253). Conversion to the bromide salt was effected by ion-exchange chromatography of [Ru(NH₃)₄(Im)₂]Cl₃ on Dowex-50 eluted with HBr followed by vacuum rotary evaporation of the solvent.

[(Im)₆Ru](ClO₄)₃ was prepared through a modification of the method of Beauchamp¹⁶ by dissolving 0.5 g of (ImH)[RuCl₄Im₂] and 1.0 g of imidazole in 10 mL of water with heating and stirring at 80 °C for 45 min until the solution turned dark red-brown. While the solution was warm, 2 g of NaClO₄ were added with stirring. The solution was filtered hot, before refrigerating overnight. The red-brown powder was collected by vacuum filtration, washed with ethanol and diethyl ether, and dried by pulling air through the frit. Anal. Calcd for [(C₅H₄N₂)₆Ru](ClO₄)₃·0.5(C₅H₄N₂): C, 27.82; H, 3.11; N, 21.63. Found: C, 27.85; H, 3.28; N, 21.57. ¹H NMR δ (ppm): H_{4,5}, -1.35, -9.0; H₂, -21.6. UV-vis (λ_{\max} nm (ϵ M⁻¹ cm⁻¹)): 203 (1.17 × 10⁵), 303 (7.88 × 10³), 401 (1.60 × 10³). E° = 295 ± 3 mV, pH 1–7. pK_{a1} = 8.5 ± 0.2, pK_{a2} = 10.8 ± 0.2.

[(1MeIm)₆Ru](PF₆)₃ and [(1MeIm)₆Ru]Cl₂·2H₂O were gifts from Procept Inc. E° for [(1MeIm)₆Ru]^{III} was measured to be 283 ± 3 mV (n = 38) between pH 1.7 and 7.5 at μ = 0.1. At pH 9.2, initial cyclic voltammetric scans yielded an E° of 273 mV; however, this decreased on subsequent scans. Diffraction studies on a few twinned crystals of [(1MeIm)₆Ru](PF₆)₃ cleaved into single crystals indicated an octahedral Ru to sit on a $\bar{3}$ site in the unit cell of the monoclinic space group $R\bar{3}$ (No. 146), with the cell parameters a = 18.36(3) Å, c = 23.47(4) Å, β = 97.89(1)°, and Z = 6; however, refinement was poor (R = 0.13).

Physical Measurements. ¹H NMR spectra were obtained in 5 mm NMR tubes on a Varian Unity 300 MHz FT spectrometer. Exchangeable protons were removed by dissolving samples (~10 mg) in D₂O followed by lyophilization (three times) before dissolution in 0.5–0.7 mL of D₂O. NMR pK_a determinations were performed by adjusting the pH (uncorrected) with dilute solutions of NaOD and DCl.

Dispersion-mode EPR spectra were collected under rapid-passage conditions at 2 K with both X-band (9.5 GHz)¹¹ and Q-band (35 GHz) spectrometers, which have been described previously.^{17,18} The advantages of using adiabatic rapid-passage conditions for broad EPR signals have been discussed.¹⁹ All complexes were dissolved (1–2 mg/mL) in a 2:1 (v:v) water/ethylene glycol mixture with the pH adjusted to 5–6 with the exception of [(1MeIm)₆Ru](PF₆)₃, which was dissolved

in 2:1 (v:v) DMF/CH₃CN. A copper background signal that originated in the cavity was digitally subtracted from all X-band spectra. Because the magnets have a limit of 1.5 T, only g values greater than 1.7 could be obtained at Q-band.

UV-vis spectra were run on a Cary 2400 spectrophotometer. Spectrophotometric pK_a determinations were made (μ = 0.1 M LiCl) by systematically varying the pH around the estimated pK_a and incorporating the absorbance data as a function of pH in the equation $pK_a = \text{pH} \pm \log[(A_{\text{pH}} - A_a)/(A_b - A_{\text{pH}})]$, where A_{pH} is the absorbance at a given pH, A_a is the absorbance of the protonated form of the complex, and A_b is the absorbance of the deprotonated form. In the case of spectral data containing evidence of two pK_a values, absorbance data were fit to the equation $A_{\text{pH}} = (A_a[\text{H}^+]^2 + A_b[\text{H}^+]K_{a1} + A_cK_{a1}K_{a2})/([\text{H}^+]^2 + [\text{H}^+]K_{a1} + K_{a1}K_{a2})$.

Electrochemistry was performed on 1–3 mM solutions in 0.1 M LiCl on a BAS 100a instrument or on a potentiostat interfaced to an IBM-PS2 running ASYST programs created in this laboratory. Reduction potentials were first examined by cyclic voltammetry to ascertain the reversibility of each couple and then measured by square wave voltammetry from peak positions relative to an internal standard, [(NH₃)₆Ru^{III}] (57 mV versus NHE). The working electrode was carbon paste, the reference electrode was Ag/AgCl, and the counter electrode was platinum wire. Pourbaix data for [(Im)₆Ru](ClO₄)₃ were fit to the equation $E_{\text{pH}} = E^\circ + 0.0591 \log\{[\text{H}^+]/([\text{H}^+] + K_{a1})\}$.

Molecular Orbital Calculations. IEHT²⁰ calculations were performed on a CACHE workstation²¹ by using crystallographic coordinates or idealized structures^{11,22} with bond distances of the following: Ru–Cl, 2.372 Å; Ru–NH₃, 2.101 Å; Ru–N_{im}, 2.048 Å. Odd-electron IEHT calculations were run as singlets using a restricted Hartree–Fock function.

Crystal Structures: *cis*-[(Im)₂(NH₃)₄Ru]Br₃. Pertinent crystal data for *cis*-[(Im)₂(NH₃)₄Ru]Br₃ are given in Table 1 with crystal coordinates listed in Table S-II (supporting information). Twinned crystals of *cis*-[(Im)₂(NH₃)₄Ru]Br₃ were grown by slow vapor diffusion of ethanol into an aqueous solution of the compound. A suitable crystal was mounted on a glass fiber, placed in the beam of a Rigaku AFC5R diffractometer, and cooled in a stream of N₂. The Ru atom and its first coordination sphere were located by direct methods using the SHELXS structure solution package.²³ The remaining non-hydrogen atoms were located from difference Fourier maps as were H atoms on C3, N3, and N4. The remaining hydrogens were placed in calculated positions (C–H = 0.95 Å, N–H = 0.87 Å) and were assigned isotropic thermal parameters, which were 20% greater than the B_{eq} value of the atoms to which they were bonded. Neutral atom scattering factors and anomalous dispersion effects were included in F_{calc} ; the values for $\Delta f'$ and $\Delta f''$ were those of Cromer.²⁴ An empirical absorption correction (ψ -scan) was applied during the refinement process, but the final absorption correction was calculated by DIFABS.²⁵

[(1MeIm)₆Ru]Cl₂·2H₂O. Crystals of [(1MeIm)₆Ru]Cl₂·2H₂O were all noticeably twinned under polarized light, but were easily cut into single crystals. These were mounted onto glass fibers and placed in the beam of a Rigaku AFC5R diffractometer. Pertinent crystal data is given in Table I with crystal coordinates listed in Table S-III (supporting information). On the basis of the systematic absences of $h0l$ ($h + l \neq 2n$) and $0k0$ ($k \neq 2n$) and the successful solution and refinement of the structure, the space group was determined to be $P2_1/n$ (No. 14). No decay correction was necessary; however, an empirical absorption (ψ) correction was applied. Scattering factors and anomalous dispersion effects were included as above. The Ru and the majority of other atoms were located by direct methods, and the remaining atoms

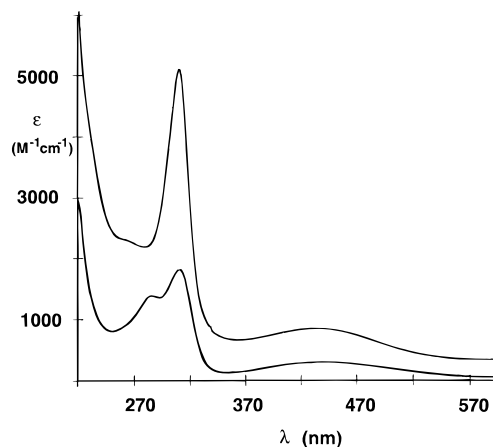
- (14) Sundberg, R. J.; Gupta, G. *Bioinorg. Chem.* **1973**, *3*, 39–48.
 (15) Pell, S. D.; Sherban, M. M.; Tramontano, V.; Clarke, M. J. *Inorg. Synth.* **1989**, *26*, 65–68.
 (16) Beauchamp, A. L.; Anderson, C. *Inorg. Chem.* **1995**, *34*, 6065–6073.
 (17) Cline, J.; Reinhammar, B.; Jensen, P.; Venters, R. A.; Hoffman, B. M. *J. Biol. Chem.* **1983**, *258*, 5124.
 (18) Werst, M. M.; Davoust, C. E.; Hoffman, B. M. *J. Am. Chem. Soc.* **1991**, *113*, 1533–1537.
 (19) Mailer, C.; Taylor, C. P. S. *Biochim. Biophys. Acta* **1973**, *322*, 195–203.

- (20) Hoffmann, R. *J. Chem. Phys.* **1963**, *39*, 1397–1412.
 (21) CACHE, ZINDO, 1991, Terra Pacific Writing Corp., Beaverton, OR 97075.
 (22) Keppler, B. K.; Wehe, D.; Endres, H.; Rupp, W. *Inorg. Chem.* **1987**, *26*, 844–846.
 (23) Sheldrick, G.; Egert, E. SHELXS/PATSEE Structure Solution Package; Institut für Anorganische Chemie der Universität Tammanstr: Göttingen, Germany, 1992.
 (24) Cromer, D. T.; Weber, J. T. *International Tables for X-ray Crystallography*; Kynoch Press: Birmingham, England, 1974; Vol. 4, Tables 2.2 A and 2.3.1.
 (25) Walker, N.; Stuart, D. *Acta Crystallogr.* **1983**, *A39*, 158–166.
 (26) Gilmore, C. J. *J. Appl. Crystallogr.* **1984**, *17*, 42–46.

Table 1. Crystallographic Data^{a,b} for *cis*-[(Im)₂(NH₃)₄Ru]Br₃ and [(1MeIm)₆Ru]Cl₂·2H₂O

formula	H ₂₀ C ₆ N ₈ Br ₃ Ru	H ₄₀ C ₂₄ N ₁₂ O ₂ Cl ₂ Ru
fw	545.06	700.64
<i>T</i> (°C)	-59(2)	-45(1)
space group, crystal system	<i>P</i> 1̄ (No. 2), triclinic	<i>P</i> 2 ₁ / <i>n</i> (No. 14), monoclinic
cell constants		
<i>a</i> (Å) =	8.961(2)	7.994(2)
<i>b</i> (Å) =	12.677(3)	13.173(4)
<i>c</i> (Å) =	7.630(2)	14.904(2)
α (deg) =	98.03(2)	90
β (deg) =	100.68(2)	97.89(1)
γ (deg) =	81.59(2)	90
cell volume (Å ³)	837.0(4)	1554.6(6)
<i>Z</i> (fw/unit cell)	2	2
crystal dimensions (nm)	0.15 × 0.05 × 0.2 (twinned)	0.30 × 0.30 × 0.40
radiation source	Cu Kα λ = 1.54 178 Å	Cu Kα λ = 1.54 178 Å
(graphite monochromated)		
<i>d</i> _{calcd} (g/cm ³)	2.163	1.497
μ (cm ⁻¹), rel trans factors	162.79, 0.79–1.89	61.53, 0.73–1.00
	0.044	0.052
$R = \frac{\sum(F_o - F_c)}{\sum F_o }$		
	0.064	0.067
$R_w = \left[\frac{\sum w(F_o - F_c)^2}{\sum w F_o ^2} \right]^{1/2}$ ^c		
	2.13	3.15
goodness of fit = $\frac{\sum w(F_o - F_c)/\sigma}{N_{\text{obs}} - N_{\text{parameters}}}$		

^a Reflections with $I_o > 3\sigma(I_o)$ were retained as observed and used in the solution and refinement of the structure. Three standard reflections were monitored with a limit of 0.2% variation. Function minimized $\sum w(|F_o| - |F_c|)^2$. ^b All calculations were performed by using the TEXSAN TEXRAY Structure Analysis Package, Molecular Structure Corp., 1985. ^c Weighting scheme: $w = 4(F_o)^2/[\sigma^2(F_o)^2]$.

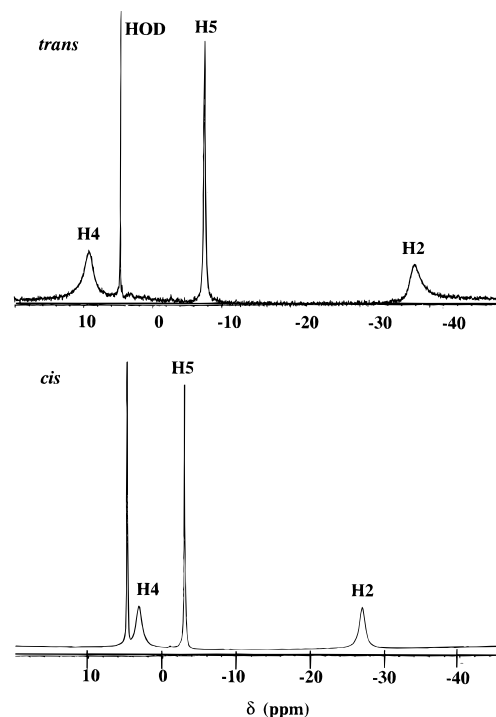
**Figure 1.** UV-vis spectra of *cis*- (bottom) and *trans*-[(Im)₂(NH₃)₄Ru]³⁺ (top) in water, pH ~ 5.

were found from difference Fourier maps.^{26,27} The non-hydrogen atoms were refined anisotropically. Hydrogen atoms were included in the structure factor calculation in idealized positions and included in the full-matrix least-squares refinement as above.

Results

Spectra and Electrochemistry. A comparison of the UV-vis and ¹H NMR spectra for *cis*- and *trans*-[(Im)₂(NH₃)₄Ru]³⁺ is shown in Figures 1 and 2, respectively. Both UV-vis and ¹H NMR spectroscopic titrations of these complexes yielded *pK_a* values for the coordinated imidazoles of 9.10 and 10.50 for the *cis* complex and 8.71 and 9.92 for the *trans* complex.

Ruthenium(III,II) reduction potentials for *cis*- and *trans*-[(Im)₂(NH₃)₄Ru]³⁺ are 0.152 and 0.121 V, respectively. When both imidazoles are deprotonated, the corresponding *E*^o values are -0.118 and -0.202 V, respectively. The reduction potentials for [(Im)₆Ru^{III,II}] and [(1MeIm)₆Ru^{III,II}] are 0.295 and 0.283 V, respectively, and are independent of pH between pH 1 and

**Figure 2.** ¹H NMR spectra of *cis*- (bottom) and *trans*-[(Im)₂(NH₃)₄Ru]³⁺ (top) in D₂O.

7.5. The Pourbaix plot for [(Im)₆Ru^{III,II}] yielded a *pK_a* for the Ru^{III} complex of 8.6, which is in reasonable agreement with the spectrophotometric *pK_a* of 8.5 determined at 316 and 400 nm. Spectrophotometric titrations monitored at 400 and 500 nm revealed *pK_{a2}* to be 10.8. Spectrophotometric evidence also indicates a third *pK_a* around 13. Since Alessio had raised a question about his reported reduction potential of *trans*-[(Im)₂Cl₄Ru^{III,II}] (-269 mV),²⁸ which appeared to be anomalously high relative to its expected value (-1.2 V) as estimated

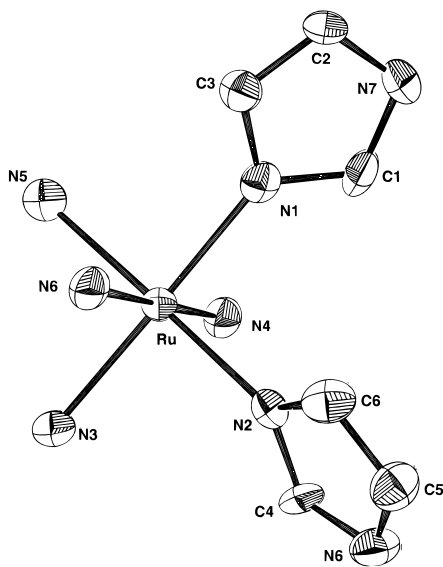


Figure 3. ORTEP diagram of *cis*-[(Im)₂(NH₃)₄Ru]³⁺.

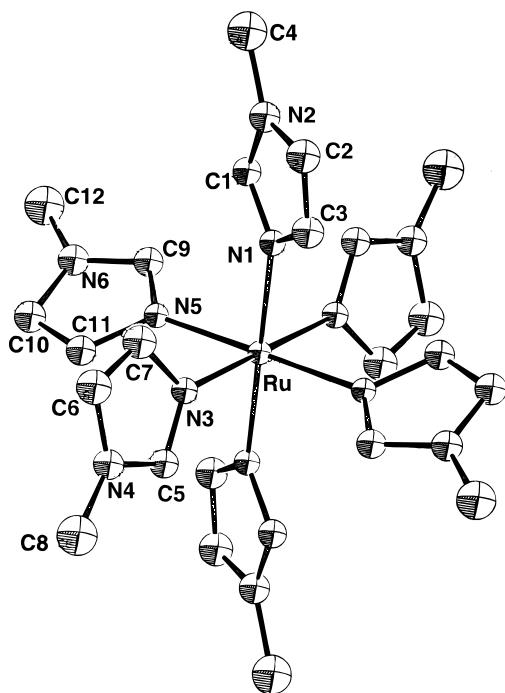


Figure 4. ORTEP diagram of [(1MeIm)₆Ru]²⁺.

by Lever's method²⁹ and others have reported an even higher value (-0.14 V),⁶ it was redetermined by square wave voltammetry on fresh solutions and new electrode surfaces to be -262 ± 6 mV ($n = 34$). Other reported reduction potentials of Ru^{III} imidazole complexes with anionic ligands are also higher than those predicted by Lever's method (e.g., *trans*-[(Im)X(NH₃)₄Ru]^{III,II}], where $E^\circ = -25$ mV, versus a Lever estimate of -227 mV, for X = SO₄²⁻ and $E^\circ = 25$ mV, versus an estimated -204 mV, for X = Cl⁻).¹¹

Structure. The structures of *cis*-[(Im)₂(NH₃)₄Ru]³⁺ and [(1MeIm)₆Ru]²⁺ are shown in Figures 3 and 4, respectively. The bond distances of nitrogens coordinated to the rutheniums in *cis*-[(Im)₂(NH₃)₄Ru]Br₃ and [(1MeIm)₆Ru]Cl₂·2H₂O are listed in Table 2. The shorter Ru–N_{Im} distances relative to the Ru–

Table 2. Selected Bond Distances (Å) around Ru for *cis*-[(Im)₂(NH₃)₄Ru]Br₃ and [(1MeIm)₆Ru]Cl₂·2H₂O

atom	<i>cis</i> -[(Im) ₂ (NH ₃) ₄ Ru]Br ₃	[(1MeIm) ₆ Ru]Cl ₂ ·2H ₂ O
	distance	distance
N1	2.05(1)	2.113(4)
N2	2.051(9)	2.108(4)
N3	2.10(1)	2.098(4)
N4	2.13(1)	
N5	2.112(9)	
N6	2.11(1)	

N_{NH₃} distances evident for the Ru^{III} complex are in concert with a number of other structural (average Ru^{III}–N_{Im} = 2.06 ± 0.02 Å) and spectroscopic studies suggesting imidazole to be a moderate π -donor ligand to Ru^{III}.^{11,22,28,30–33} This effect is not evident in the Ru^{II} structure as the low-spin d⁶ electronic configuration prevents the metal from accepting π -electron density from the imidazole. While the reduction potentials for these complexes and the reported Lever electrochemical parameter for imidazole suggest that it can also serve as a π -acceptor ligand (see below), in the absence of strong π -donor ligands this effect is weak, so that the Ru^{II}–N_{Im} distances are very near Ru^{II}–N_{NH₃} distances (2.114(4) Å).³⁴ The average Ru–N_{Im} bond distance of the three crystallographically independent imidazoles in [(1MeIm)₆Ru]Cl₂·2H₂O (2.106(8) Å) is identical within experimental error with that reported for [(Im)₆Ru]CO₃·5H₂O (2.102(2) Å).¹⁶

In *cis*-[(Im)₂(NH₃)₄Ru]^{III}]Br₃ the imidazole ring containing N1 is planar with a mean deviation of 0.01 Å and is canted at an angle of 36.6° to the plane formed by N1, N3, N4, and N6. The ring containing N2 is planar within a mean deviation of 0.0015 Å and forms an angle of 43.6° with the plane defined by N2, N4, N5, and N6. The angle between the two imidazole planes is 112.5°. There is no significant stacking of the imidazole rings.

In [(1MeIm)₆Ru]Cl₂·2H₂O, an inversion center causes opposite imidazoles to be in the same plane. The plane of each imidazole is roughly 90° from those of the adjacent imidazoles. Mean deviations from the plane of the imidazoles ligated through N1, N3, and N5 are 0.0025, 0.0048, and 0.0008 Å, respectively.

EPR and ¹H NMR Spectroscopies. EPR measurements and ligand field parameters are summarized in Table 3, and proton NMR data are listed in Table 4. The g values obtained for all ammine complexes in frozen solution match the corresponding solid complex g values, suggesting that the low-temperature frozen solution structure is the same as the solid state structure. The EPR and ligand field parameters (Table 3) were analyzed by a previously described procedure¹¹ on the basis of several mathematical approaches for handling low-spin d⁵ systems.^{35–40}

Since the calculated g_3 value for [(1MeIm)₆Ru^{III}] (Table 3) was not observed at X- or Q-band fields and the Q-band EPR

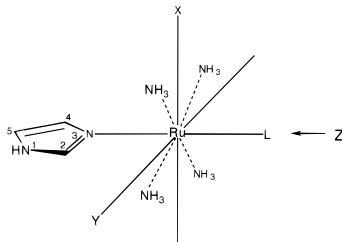
- (27) Beurskens, P. T. *DIRDIF*, Technical Report; Crystallographic Laboratory: Toernooiveld, Nijmegen, The Netherlands, 1984.
 (28) Alessio, E.; Balducci, G.; Lutman, A.; Mestroni, G.; Calligaris, M.; Attia, W. M. *Inorg. Chim. Acta* **1993**, *203*, 205–217.
 (29) Lever, A. B. P. *Inorg. Chem.* **1990**, *29*, 1271–1285.

- (30) Wishart, J. F.; Zhang, X. A.; Isied, S. S.; Potenza, J. A.; Schugar, H. J. *Inorg. Chem.* **1992**, *31*, 3179–3181.
 (31) Krogh-Jespersen, K.; Westbrook, J. D.; Potenza, J. A.; Schugar, H. J. *J. Am. Chem. Soc.* **1987**, *109*, 7025–31.
 (32) Calligaris, M.; Faleschini, P.; Todone, F.; Allesio, E.; Geremia, S. *J. Chem. Soc., Dalton Trans* **1995**, 1653–1662.
 (33) Sudha, C.; Mandal, S. K.; Chakravarty, A. R. *Inorg. Chem.* **1993**, *32*, 3801–3802.
 (34) Stynes, H. C.; Ibers, J. A. *Inorg. Chem.* **1971**, *10*, 2304–2308.
 (35) Bleaney, B.; O'Brien, M. C. M. *Proc. Phys. Soc. B (London)* **1956**, *69*, 1216–1230.
 (36) Bohan, T. L. *J. Magn. Reson.* **1977**, *26*, 109–118.
 (37) Griffith, J. S. *Mol. Phys.* **1971**, *21*, 135–139.
 (38) Kotani, M. in *The Structure and Properties of Biomolecules and Biological Systems*; Duchesne, J., Ed.; Interscience: London, 1964; pp 159–181.

Table 3. EPR g Values and Estimated Crystal Field Splitting Energies and State Energies in Units of λ for Ruthenium(III) Complexes with Imidazole Ligands^a

ligands	g_1 (g_1 calcd)	axes	g_2 (g_2 calcd)	axes	g_3 (g_3 calcd)	axes	Δ^c	$ V ^d$	ϵ_1^e	ϵ_2	ϵ_3
Im(NH ₃) ₅	2.98 (2.99)	z	2.02 (-2.02)	y	(0.61)	x	-0.79	0.44	-0.62	0.74	1.33
1MeIm(NH ₃) ₅	2.92 (2.92)	z	2.09 (-2.09)	y	(0.63)	x	-0.72	0.46	-0.63	0.74	1.29
2MeIm(NH ₃) ₅	2.90 (-2.90)	z	2.18 (2.18)	y	(0.51)	x	0.76	0.44	-0.60	0.79	1.33
5MeIm(NH ₃) ₅	2.88 (-2.86)	z	2.19 (2.19)	y	(0.54)	x	0.74	0.42	-0.61	0.78	1.30
<i>cis</i> -(Im) ₂ (NH ₃) ₄	2.88 (-2.87)		2.14 (2.14)		(0.65)		0.69 ^f	0.42	-0.63	0.76	1.26
<i>trans</i> -(Im) ₂ (NH ₃) ₄	3.04 (3.05)	z	2.20 (-2.18)	y	(0.15)	x	0.97	0.63	-0.52	0.88	1.60
<i>trans</i> -(Im) ₂ Cl ₄ ^p	3.08 (-3.05)		2.38 (2.34)		(1.10)		2.03	0.62	-1.65	0.13	1.52
<i>trans</i> -(Im ⁻) ₂ (NH ₃) ₄ ^g	2.54 (-2.57)		2.46 (2.46)		1.54 (-1.57)		2.8	0.4	-0.20	2.86	3.75
1MeIm ₆	2.48 (-2.48)	\perp	2.48 (2.48)	\perp	(1.75)	$\parallel(z)$	3.75	0.0	-0.16	3.40	4.25

^a Axis system for ammineruthenium(III) imidazole complexes (z -axis for hexaimidazole complexes is taken to be the trigonal axis):



^b 3.13, 2.44, and 1.2 according to ref 6. ^c Value for electron (rather than hole) formalism. ^d The sign of V has been arbitrarily taken as positive. ^e Values of ϵ_j are given relative to T_1 , the lowest lying ligand field configuration in the hole model. ^f A previous assignment of a large Δ in *cis*-[(Im)₂(NH₃)₄Ru^{III}]³⁺, which was based on an erroneous assignment of the g_3 value,¹¹ has been changed to be more in line with those of similar complexes. ^g Fully deprotonated bis-imidazolato complex. (Calculated values were obtained by using $k = 0.89$.) Taken from ref 11.

line shape of this complex closely matches that of *trans*-[(Im)₂(NH₃)₄Ru^{III}], in which a g_3 value of 1.54 is readily observed, the same covalency reduction parameter ($k = 0.89$) was used in fitting the g_{\perp} value (2.48) for [(1MeIm)₆Ru^{III}]. The resulting values for Δ (3.0) and g_3 (calcd) are more reasonable and more in line with the other complexes. Only one g value (2.67) could be measured for the carbon-bound complex *trans*-[Cl(Im κ ^{C2})(NH₃)₄Ru^{III}]Cl₂ with a second being evident, but out of range of the magnet.

¹H NMR peak assignments in these complexes were made with the aid of the inverse relationships between the distance from the metal ion and the line shifts and the line broadening.⁴¹⁻⁴⁴ Assignments were verified by systematic methylation of the ligands and are in accord with those of the histidyl imidazole in pentaammineruthenium(III) myoglobin.⁴¹ The H2 assignments are also consistent with those for the analogous proton (H8) in corresponding purine complexes.⁴³ This resonance has the broadest line width and is always shifted substantially upfield relative to the free ligand (cf., isotropic shift (δ_{iso}) values in Table 4). The H4 resonance is broadened to about the same degree as H2 but may be shifted either upfield or downfield, depending on the site of methylation. The H5 resonance is the least broadened, but the paramagnetic effect always results in a significant upfield shift. Ionization of the imidazole increases the upfield shift for both H2 and H5 and enhances line broadening for all resonances. Since ionization increases π -donation from the imidazole, these effects can be attributed to increased transfer of spin density to the heterocycle.

As expected, the methyl protons at any given position are generally shifted in the opposite direction from the correspond-

ing ring proton.⁴⁴⁻⁴⁶ Methylation at C2 results in a large downfield shift for the methyl protons and an upfield shift for H5, which is only 2.5 ppm upfield from the δ_{iso} (H5) of the parent complex; however, a substantial downfield shift becomes evident for H4. These relative changes increase upon ionization of the imidazole ring. A similar situation holds for (what is considered to be) methylation at C4, where the δ (H2) shifts 6.3 ppm downfield from the parent complex. On the other hand, methylation at N1 leads to an upfield shift for H4, similar to that for the parent complex.

The isotropic shifts (δ_{iso}) listed in Table 4 represent the shift induced by the metal ion through a combination of contact and pseudocontact (dipolar) interactions. The dipolar component (δ_{dip}) of the isotropic shift was estimated according to the following equation for an $S = 1/2$ electron spin system at 292 K:

$$\delta_{dip} = \frac{\Delta\nu_{dip}}{\nu} = \frac{177.6}{r^3} \left\{ (3 \cos^2 \theta - 1) \left(g_z^2 - \frac{g_x^2 + g_y^2}{2} \right) + \frac{3}{2} \sin^2(\theta) \cos(2\phi) (g_y^2 - g_x^2) \right\}$$

where r (Å) is the Ru-H distance, θ is the angle formed by the Ru-H vector and the Ru-N_{im} axis, ϕ is the angle from the x -axis of the Ru-H vector projected onto the xy -plane with $\cos(2\phi) \approx -1$, and the g values are given in Table 3 for the compounds studied.⁴⁶ The axis system for the ammine imidazole complexes is shown in Table 3. Wherever rotational effects are significant or ϕ could not be reasonably estimated, no values for δ_{dip} or δ_{con} are given. As the z -axis in the hexaimidazole complexes was taken as the crystallographic trigonal ($\bar{3}$) axis, accurate values of θ could not be estimated owing to the possibility of a 180° disorder between the C2 and C4 positions in solution.

Rotation about the z -axis should have a negligible effect on H5 ($\theta = 15^\circ$), but generates a greater effect on the paramagnetic field for both H4 and H2 ($\theta = 40^\circ$). The comparison of δ_{iso}

(39) Taylor, C. P. S. *Biochim. Biophys. Acta* **1977**, *491*, 137-149.

(40) Weissbluth, M. In *Hemoglobin*; Springer-Verlag: New York, 1974; pp 99-105.

(41) Toi, H.; LaMar, G. N.; Margalit, R.; Che, C. M.; Gray, H. B. *J. Am. Chem. Soc.* **1984**, *106*, 6213.

(42) *NMR of Paramagnetic Molecules*; La Mar, G. N., Horrocks, W. D., Holm, R. H., Eds.; Academic Press: New York, 1973, p 667ff.

(43) Rodriguez-Bailey, V. Ph.D. Thesis, Boston College, Chestnut Hill, MA, 1992.

(44) Bertini, I.; Luchinat, C. In *Physical Methods in Chemistry*, 2nd ed.; Drago, R. S., Ed.; W. B. Saunders Co.: Philadelphia, PA, 1992; pp 500-566.

(45) La Mar, G. N.; Horrocks, W. D.; Allen, L. *J. Chem. Phys.* **1964**, *41*, 2126-2134.

(46) Bertini, I.; Luchinat, C. *NMR of Paramagnetic Molecules in Biological Systems*; Benjamin Cummings: San Francisco, CA, 1986, pp 36-38.

Table 4. ^1H NMR Shifts for Ruthenium(III) Complexes with Imidazole Ligands

ligands	coord site	ioniz site	proton	δ (ppm)	δ_{dia}^a (ppm)	δ_{iso} (ppm)	δ_{dip} (ppm)	δ_{con} (ppm)	T_1^b (ms)
Im(NH ₃) ₅	3		H2	-27.0	7.54	-34.6			0.96
			H4	3.2	6.90	-3.7			1.61
			H5	-3.0	6.90	-9.9	14.6	-24.5	9.65
Im ⁻ (NH ₃) ₅	3	1	H2	-29.2	7.49	-36.7			0.59
			H4	3.1	6.93	-3.8			0.88
			H5	-8.5	6.93	-15.4			1.33
1MeIm(NH ₃) ₅	3		CH ₃ (1)	25.4	3.51	21.9			1.33
			H2	-28.7	7.41	-36.1			
			H4	3.1	6.86	-3.8			1.33
2MeIm(NH ₃) ₅	3		H5	-4.0	6.91	-10.9	13.4	-24.4	
			CH ₃ (2)	57.5	2.10	55.4			1.27
			H4	17.5	6.83	10.7			
2MeIm ⁻ (NH ₃) ₅	3	1	H5	-5.6	6.83	-12.4	13.7	-26.1	0.84
			CH ₃ (2)	63.7	2.13	61.5			
			H4	20.3	6.75	13.5			
5MeIm(NH ₃) ₅	3		H5	-17.4	6.75	-24.2			
			H2	-40.3	7.43	-47.8			0.91
			H4	9.4	6.61	2.8			1.06
5MeIm ⁻ (NH ₃) ₅	3	1	CH ₃ (5)	19.0	2.01	16.9	-11.4	28.3	1.28
			H2	-45.2	7.41	-52.6			
			H4	12.5	6.63	5.9			
<i>cis</i> -(Im) ₂ (NH ₃) ₄	3		CH ₃ (5)	29.4	2.04	27.4			
			H2	-27.1	7.54	-34.6			
			H4	3.2	6.90	-3.7			
<i>cis</i> -(Im ⁻) ₂ (NH ₃) ₄	3	1	H5	-3.0	6.90	-9.9			
			H2	-35.6	7.49	-43.1			
			H4	9.2	6.93	2.3			
<i>trans</i> -(Im) ₂ (NH ₃) ₄ ^c	3		H5	-25.1	6.93	-32.0			
			H2	-37.8	7.54	-45.3			
			H4	9.3	6.90	2.4			
<i>trans</i> -(Im ⁻) ₂ (NH ₃) ₄ ^d	3	1	H5	-7.4	6.90	-14.3	14.8	-29.1	
			H2	-46.1	7.49	-53.6			
			H4	12.4	6.93	5.5			
<i>trans</i> -(Im) ₂ Cl ₄ ^e	3		H5	-36.3	6.93	-43.2			
			H2	-21.0	7.54	-28.5			
			H4	-16.0	6.90	-22.9			
Im ₆	3		H5	-5.7	6.90	-12.6	13.2	-25.8	
			H2	-21.6	7.54	-29.1			
			H4	-1.4	6.90	-8.3			
1MeIm ₆	3		H5	-9.0	6.90	-15.9			
			CH ₃ ^e	12.2	3.51	8.7			
			H2	-18.5	7.41	-25.9			
<i>trans</i> -(Im)Cl(NH ₃) ₄	2		H4	-1.6	6.86	-8.4			
			H5 ^f	0.8	6.91	-6.2			
			H4,5	-14.8	6.90	-21.7			8.49
<i>trans</i> -(Im)H ₂ O(NH ₃) ₄	2		H4,5	-35.3	6.90	-42.2			2.83
<i>trans</i> -(Im)HO(NH ₃) ₄	2		H4,5	-15.6	6.90	-22.5			

^a Free ligand values. ^b $\Delta\nu_{1/2}$ was measured from the NMR peak by the triangulation method. The relaxation time was estimated as $T_1 = T_2 = 1/\pi\Delta\nu_{1/2}$. ^c Taken from ref 11. ^d Taken from refs 6 and 54. ^e Doublet, $J = 180$ Hz. ^f Quartet, $J = 42$ Hz.

values for [(Im)(NH₃)₅Ru^{III}] and the corresponding complexes with 2MeIm,⁴³ which is sterically hindered from rotating, revealed that H5 is shifted 2.5 ppm upfield with 2MeIm relative to Im (cf., Table 4). In contrast with this, there is a 14.4 ppm downfield change relative to the parent (rotating Im) complex when H4 is sterically constrained to lie between the *cis*-ammines in 2MeIm. Preliminary studies to treat imidazole rotation exactly show that, while the predicted effects of such rotation on the ground electronic states of these compounds are extremely complicated, the present treatment yields good estimates for δ_{dip} for H5. Even so, an exact calculation of δ_{dip} values for the 5-methyl protons remains difficult,⁴⁷ yet these are certainly of the same sign as that for H5. As the out-of-plane angles for the Ru-H_{CH₃} vectors are no more than $\sim 5^\circ$ from the Ru-H(5) vectors, $\delta_{\text{dip}}(\text{CH}_3(5))$ was estimated at the average position of the methyl hydrogens.

C-Bound Complexes. The spectra of the C2-bound (imidazolylidene) complexes of imidazole are complicated by the

kinetic *trans* effect generated by these ligands^{12,13} which causes water exchange of the inner-sphere chloride. Consequently, these spectra vary with time, chloride concentration, and, especially for the aqua complexes, pH. In these complexes, H4 and H5 are symmetry related, so that only a single resonance is observed, which is approximately the same (~ -22 ppm) for both the *trans*-chloro and *trans*-hydroxo complexes.^{12,13} Protonation to yield the *trans*-aqua species shifts the latter resonance an additional 20 ppm upfield. The peak assigned to the *trans*-chloro complex was identified by adding NaCl, which increased the intensity of the peak at -14.8 ppm and decreased that at -35.3 ppm. As spectra of the ylidene tautomeric form of the free ligands are not available, δ_{iso} values are calculated from the prevalent tautomer.

Discussion

Spectra. A comparison of the spectrum shown in Figure 1 with that listed by Sundberg for [(Im)₂(NH₃)₄Ru]³⁺ reveals the previously reported complex, which was formed by allowing [(Im)(NH₃)₅Ru]²⁺ to stand in acid,¹² to be the *trans* isomer rather

than the *cis* isomer. By implication $[(1,3\text{Me}_2\text{Xan})_2(\text{NH}_3)_4\text{Ru}]^{3+}$, which is similarly prepared, is also likely to have a *trans* geometry.¹³ The two maxima evident in the near-UV spectrum of the *cis* isomer (relative to one in the *trans* spectrum) probably derive from d_{xz} and $d_{x^2-y^2}$ being nearly equivalent prior to spin-orbit interactions, since each interacts with an imidazole π orbital.

For the *cis*- and *trans*-bisimidazole complexes, respectively, the differences between the first and second ionization constants ($\Delta pK_{a1,2} = pK_{a2} - pK_{a1}$; $\Delta pK_{a1,2-cis} = 1.3 \pm 0.1$, $\Delta pK_{a1,2-trans} = 1.1 \pm 0.1$) are greater than the statistical value of 0.60 expected in noninteracting diprotic ionization sites⁴⁸ but less than that in conjugated dicarboxylic acids ($\Delta pK_a(\text{fumaric}) = 1.5$; $\Delta pK_a(\text{oxalic}) = 2.8$) or oxo inorganic acids ($\Delta pK_a = \sim 5$). In the case of $[(\text{Im})_6\text{Ru}]^{3+}$, $\Delta pK_{a1,2}$ and $\Delta pK_{a2,3}$ are both ~ 2.2 , which is also significantly greater than the statistical difference (0.38) expected between the first two pK_a values of a hexaionizable complex. In all these complexes, some of the contribution to $\Delta pK_{a1,2}$ is probably due to electronic communication between the imidazole ligands mediated through the metal d_π orbitals.

While the NMR spectra of the *cis* isomer of $[(\text{Im})_2(\text{NH}_3)_4\text{Ru}]^{3+}$ is very similar to that of $[(\text{Im})(\text{NH}_3)_5\text{Ru}]^{3+}$ (cf., Figure 2 and Table 4), that of the *trans* configuration is distinctly different.¹¹ These differences arise not only from the different geometric position of the heterocyclic protons in the magnetic field of the Ru^{III} but also from their π interactions with different d_π orbitals. In addition, *trans*- $[(\text{Im})_2(\text{NH}_3)_4\text{Ru}]^{3+}$ shows a greater ligand field splitting of the t_{2g} orbitals than does the *cis*-bisimidazole complex (cf., Δ values in Table 3), leading to a greater quenching of the spin-orbit mixing of these orbitals in the corresponding *trans* complex. The result is a ground state in the *trans* complex that has a higher percentage of the unpaired spin in the d_π orbital than the ground state in the *cis* complex. The differences observed between the *cis* and *trans* isomers in their NMR and electronic spectra should facilitate such assignments in polypeptide and nucleic acid complexes of Ru^{III} and Os^{III} , in which cross-links of both types are conceivable.^{1,49}

Electrochemistry. The reduction potentials for the hexaimidazole ruthenium(III) complexes and similar data¹¹ for *cis*- and *trans*- $[(\text{Im})_2(\text{NH}_3)_4\text{Ru}^{\text{III}}]^{3+}$ suggests that the Lever electrochemical parameter (E_L) for imidazole in ammine or imine complexes should be around 0.09 rather than 0.12.²⁹ On the other hand, for complexes with anionic ligands^{11,28} a significantly higher value for $E_L(\text{Im})$ (0.28) seems more appropriate. This may reflect the ability of the imidazole ligand to function as a weak π -donor in the presence of π -acceptor or noninteracting π ligands and as a π -acceptor in the presence of anionic, π -donor ligands. This is reasonable since the anionic ligands raise the energy of the Ru^{III} d orbitals such that the d_π orbitals become closer in energy to the imidazole π^* orbitals resulting in greater π - d_π interaction.¹¹ This is substantiated by a comparison of IEHT calculations, which show substantial $\pi^*_{\text{Im}}-d_{xz}$ mixing in *trans*- $[(\text{Im})_2\text{Cl}_4\text{Ru}^{\text{III}}]$, such that d_{xz} becomes partially bonding in character, whereas significant mixing is not evident in *trans*- $[(\text{Im})_2(\text{NH}_3)_4\text{Ru}^{\text{III}}]$. Anion expansion of the d orbitals, coupled with the imidazoles serving as an electron sink, may facilitate the apparent proton-coupled process that has been reported for this complex.⁶

Since complexes with imidazole ligands appear to be particularly effective at inhibiting T cell proliferation (e.g., the IC_{50} for *cis*- $[(\text{Im})_2(\text{NH}_3)_4\text{Ru}]^{3+}$ is 3 nM against CD4+ T cells),¹⁰

the ability of imidazole ligands to stabilize Ru^{II} may be biologically significant and raises the possibility of a redox pathway that may act in synergy with inhibition of cyclin-dependent kinases. Indeed, since at present only ruthenium complexes are active as metalloimmunosuppressants and the most active have reduction potentials between 100 and 400 mV, electron-transfer is probably involved in their activity. A likely site of metabolic interference is the respiratory redox pathway, whose ATP production is essential to cell growth.

Structure. Since metal ions may bind histidyl imidazoles through either N_δ ($N1$ in the present numbering system) or N_ϵ ($N3$), it is possible that metal cross-links in α -helical polypeptides may utilize both nitrogens.^{7,8,50} In the case of cross-links formed by *cis*- $[(\text{H}_2\text{O})_2(\text{NH}_3)_4\text{Ru}^{\text{III}}]$, the structure of *cis*- $[(\text{Im})_2(\text{NH}_3)_4\text{Ru}^{\text{III}}]^{3+}$ offers some insight into which may be preferred. The distance between the two coordinated imidazole ring nitrogens is 2.90(1) Å, and the distances between the imidazole C4 and C5 (ring numbering) sites on either ring are the following: C4-C4', 5.97(2) Å; C4-C5', 4.82(2) Å; C5-C4', 5.46(2) Å; C5-C5', 4.17(2) Å. Consequently, the best cross-linking situation for the structure exhibited here to accommodate the 5.4 Å pitch of the α -helix^{7,51} would be between the N_δ of one imidazole and the N_ϵ of another. While a preference for histidyl N_ϵ binding is expected on a steric basis, N_δ binding is quite possible. Indeed, the evidence presented for N_ϵ binding is based upon electronic spectra,^{12,14} which do not distinguish between N-bound isomers. The ^1H NMR of $[(5\text{MeIm})(\text{NH}_3)_5\text{Ru}^{\text{III}}]^{3+}$, which was purified by column ion-exchange chromatography, suggests that both the 5MeIm and 4MeIm isomers are present in a ratio of approximately 20:1 ($N_\epsilon:N_\delta$).³ Finally, the NMR spectra of these cross-links (see below) are consistent with those expected for N_ϵ -Ru- N_δ cross-links.

^1H NMR and EPR Spectra. Because of the effects of imidazole substituents and other ligands, care must be taken in assigning ring proton resonances to take both peak broadening and peak position into account. While the δ_{iso} values of the H2 and H5 imidazole protons are invariably upfield and consistent in relative magnitude with $\text{H2} > \text{H5}$ and the relative line broadening is generally $\text{H2} \geq \text{H4} \gg \text{H5}$, the relative positions of the H4 and H5 resonances in *trans*- $[(\text{Im})_2(\text{NH}_3)_4\text{Ru}^{\text{III}}]^{3+}$ are inverted relative to those in *trans*- $[(\text{Im})_2\text{Cl}_4\text{Ru}^{\text{III}}]^-$ (cf., Table 4). IEHT calculations show that in *trans*- $[(\text{Im})_2\text{Cl}_4\text{Ru}^{\text{III}}]$, the energies of all four imidazole π^* orbitals lie between the ruthenium t_{2g} and e_g levels, with a minimum energy separation ($t_{2g}-\pi^*$) of 1.62 eV. In contrast, only one imidazole π^* level lies in between the t_{2g} and e_g levels in *trans*- $[(\text{Im})_2(\text{NH}_3)_4\text{Ru}^{\text{III}}]$ with a much larger (4.13 eV) $t_{2g}-\pi^*$ energy separation. Consequently, in *trans*- $[(\text{Im})_2\text{Cl}_4\text{Ru}^{\text{III}}]$, the four chloro ligands raise the energy of the t_{2g} orbitals such that d_{xz} interacts with an imidazole π^* orbital so that the IEHT ordering of the t_{2g} orbitals is $d_{xy} > d_{yz} > d_{xz}$, whereas in the tetraammine case the ordering is $d_{xz} > d_{yz} > d_{xy}$, which may account for the changes in the proton resonances between the two complexes.

In $[(1\text{MeIm})_6\text{Ru}^{\text{III}}]^{3+}$, coupling between the methyl and C5 protons aids in assigning the resonances; however, δ_{iso} for H4 and H5 again inverts between $[(\text{Im})_6\text{Ru}^{\text{III}}]^{3+}$ and $[(1\text{MeIm})_6\text{Ru}^{\text{III}}]^{3+}$, so that alkylation studies as a means of assigning resonances must be interpreted cautiously. As often happens, the methyl proton resonances are shifted in the direction opposite the proton at the same ring position. This is due to a direct

(48) Clark, J.; Perrin, D. D. *Q. Rev.* **1964**, *18*, 300.

(49) Clarke, M. J. In *Metal Complexes in Cancer Chemotherapy*; Keppler, B. K., Ed.; VCH: Weinheim, 1993; pp 129-157.

(50) Tainer, J. A.; Getzoff, E. D.; Beem, K. M.; Richardson, J. S. *J. Mol. Biol.* **1982**, *160*, 181-217.

(51) Branden, C.; Tooze, J. *Introduction to Protein Structure*; Garland Publishing, Inc.: New York, NY, 1991.

(rather than polarized) transfer of spin density onto the methyl protons through their 1s orbitals overlapping with spin delocalization through the π system at the substituted carbon.⁵²

Methyl substitution at C2 in the pentaammine complexes, which hinders rotation of the ring, results in a pronounced downfield shift in $\delta_{\text{iso}}(\text{H4})$ which is shifted upfield in the complexes of Im and 1MeIm and somewhat downfield with 5MeIm (cf., δ_{iso} values in Table 4). The uncharacteristic downfield shift of the $\delta_{\text{iso}}(\text{H4})$ upon C2 methylation may be accounted for by a combination of steric and electronic effects. Electron donation involving the methyl group would enhance electron density at N3 and π bonding to the Ru. A C2-methyl group would also cause steric bending of the Ru–N3 bond to position the Ru closer to H4, which sits very near an octahedral face of the metal ion. Such steric modulation of a direct interaction between H4 and a ruthenium t_{2g} orbital would have a pronounced effect on the contact interaction.

In some cases it has been assumed that ruthenium labeling of histidyl imidazole sites on proteins occurs at the imidazole N_{ϵ} (N_3) site; however, the existence of two sets of resonances for $[\text{5MeIm}(\text{NH}_3)_5\text{Ru}^{\text{III}}]$ suggests that the imidazole ring of histidine can also coordinate $[(\text{NH}_3)_5\text{Ru}^{\text{III}}]$ at N_{δ} (N_1). Indeed, the evidence presented for N_{ϵ} -coordination in $[(\text{His})(\text{NH}_3)_5\text{Ru}^{\text{III}}]$ is based upon electronic spectra,^{12,14} which would not distinguish between N-coordinated linkage isomers. This is a significant consideration in studies involving long-range electron transfer to Ru sites on proteins, since binding at N_{δ} would change the overlap function at C5.⁵³ In a recent approach to stabilizing α -helices by cross-linking His-imidazoles through binding cis - $[(\text{H}_2\text{O})_2(\text{NH}_3)_4\text{Ru}^{\text{III}}]$, N_{ϵ} binding has also been assumed. However, the crystal structure of $[(\text{Im})_2(\text{NH}_3)_4\text{Ru}]\text{Br}_3$ suggests that the best cross-linking situation to accommodate the 5.4 Å pitch⁵¹ of the α -helix⁷ involves binding the N_{δ} of one imidazole and the N_{ϵ} of a second.¹¹ In cross-linking α -helices through cis - $[(\text{His})_2(\text{NH}_3)_4\text{Ru}^{\text{III}}]^{3+}$, broad ^1H NMR peaks at 0.56 and -0.78 ppm have been noted.⁷ Since neither of these occurs in the range expected for H2 (-20 to -30 ppm), the two resonances probably arise from H4 in two different environments, which may result from the two linkage isomers.

The dipolar shifts are sufficiently large to be of help in ascertaining the binding of these complexes to proteins and thereby determine their mode of action in anticancer or anti-T-cell therapies. For example, in $[(\text{Im})(\text{NH}_3)_5\text{Ru}^{\text{III}}]$ at 7 Å, δ_{dip}

ranges from -0.5 to 6.55 ppm, depending on the angle from the z -axis. This, coupled with the high anisotropy and magnetic relaxation effects should make it possible to map the binding geometry with nonrotating Ru^{III} imidazole complexes.

C-Bound Imidazole. For the *trans*-chloro, *trans*-aqua, and *trans*-hydroxo C2-bound imidazolylidene complexes, an inverse relationship exists between the π -donating properties of the ligand *trans* to the ylidene (chloride \geq hydroxide $>$ aqua) and both the chemical shift and line broadening. The stronger the π -donor interaction of the *trans* ligand, the weaker the π -donor interaction of the imidazolylidene, which decreases the amount of π spin density transferred onto the heterocycle and thus decreases the paramagnetic contact interactions.

Conclusions. While imidazole can serve as a weak π -donor ligand,¹¹ it may also serve as a significant π -acceptor when anionic ligands are present. The excellent immunosuppressant activities of the ruthenium immunosuppressant drugs, such as *cis*- $[(\text{Im})_2(\text{NH}_3)_4\text{Ru}^{\text{III}}]\text{Cl}_3$ and $[(\text{Im})_6\text{Ru}^{\text{III}}]\text{Cl}_3$, may well be due to the imidazole ligands tuning the $\text{Ru}^{\text{III,II}}$ reduction potential to a range optimal for biological activity, yet retaining a fairly small size that can readily interact with redox sites in proteins. In keeping with the biological properties of the Ru immunosuppressants being exquisitely dependent on their electronic properties, the UV–vis, ^1H NMR, and EPR spectra of these complexes are sensitive to small structural and electronic perturbations. Such spectroscopic differences should also readily distinguish between *cis* and *trans* cross-linking to imidazole rings in both proteins and nucleic acids. When an alkyl group is at C4 or C5, the ^1H NMR appears to discriminate between imidazole N_{δ} and N_{ϵ} coordination that may occur on histidyl imidazoles in proteins. The EPR and NMR parameters reported here should make it possible to utilize these sorts of complexes as probes for elucidating some of the factors that contribute to the efficacy of both the anticancer and immunosuppressant ruthenium drugs.

Acknowledgment. This work was supported by NIH Grant GM26390 at Boston College and by NIH HL13531 at Northwestern University. We thank Hans Van Willigen (University of Massachusetts, Boston) for preliminary EPR results.

Supporting Information Available: Pourbaix plot for $[(\text{Im})_6\text{Ru}^{\text{III,II}}]$ in aqueous solution, $\mu = 0.1$ LiCl, complete crystallographic tables for *cis*- $[(\text{Im})_2(\text{NH}_3)_4\text{Ru}]\text{Br}_3$ and $[(1\text{MeIm})_6\text{Ru}]\text{Cl}_2 \cdot 2\text{H}_2\text{O}$, and ground state (ϵ_i) coefficients of the hole states for imidazole complexes of Ru^{III} and percentage hole character in the d_{xz} orbital (21 pages). Ordering information is given on any current masthead page.

IC960355C

(52) Bertini, I.; Luchinat, C. In *Physical Methods for Chemists*, 2nd ed.; Drago, R. S., Ed.; Saunders: Ft. Worth, TX, 1992; pp 500–558.

(53) Beratan, D. N.; Onuchic, J. N.; Betts, J. N.; Bowler, B. E.; Gray, H. B. *J. Am. Chem. Soc.* **1990**, *112*, 7915–21.

(54) Anderson, C.; Beauchamp, A. L. *Can. J. Chem.* **1995**, *73*, 471–482.